FISEVIER

Contents lists available at ScienceDirect

Science of the Total Environment

journal homepage: www.elsevier.com/locate/scitotenv



Spatial and temporal variations of microplastic concentrations in Portland's freshwater ecosystems



Rebecca Talbot ^a, Elise Granek ^b, Heejun Chang ^{a,*}, Rosemary Wood ^b, Susanne Brander ^c

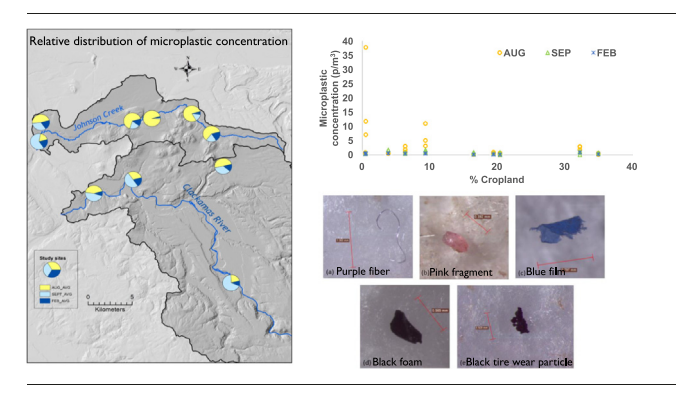
- ^a Department of Geography, Portland State University
- ^b Department of Environmental Science and Management, Portland State University
- ^c Department of Fisheries, Wildlife, and Conservation Sciences; Coastal Oregon Marine Experiment Station, Oregon State University

HIGHLIGHTS

Lower water velocity rates may have facilitated the accumulation of microplastics.

- Nearstream analyses explained more MP concentrations than watershed analyses.
- Larger size microplastics dominated in the high-flow event samples.
- Fragments were the dominant microplastic morphology observed.
- Polyethylene was the dominant polymer type, followed by polypropylene.

GRAPHICAL ABSTRACT



ARTICLE INFO

Editor: Thomas Kevin V

Keywords:
Microplastics
Freshwater pollution
Land use
Precipitation
Scale
GIS

ABSTRACT

While microplastics are a pollutant of growing concern in various environmental compartments, less is known regarding the sources and delivery pathways of microplastics in urban rivers. We investigated the relationship between microplastic concentrations and various spatiotemporal factors (e.g., land use, arterial road length, water velocity, precipitation) in two watersheds along an urban-rural gradient in the Portland metropolitan area. Samples were collected in August, September, and February and were analyzed for total microplastic count and type. Nonparametric statistics were used to evaluate potential relationships with the explanatory variables, derived at both the subwatershed and near stream scales. In August, microplastic concentrations were significantly higher than in February. August concentrations also negatively correlated with flow rate, suggesting that lower flow rates may have facilitated the accumulation of microplastics. Smaller size microplastic particles (< 100 µm) were found more in August than September and February, while larger size particles were more dominant in February than the other months. Microplastic concentrations were positively related to 24-h antecedent precipitation in February. Negative correlations existed between wet season microplastic concentrations and agricultural lands at the near stream level. The results indicate that near stream variables may more strongly influence the presence and abundance of microplastics in Portland's waterways than subwatershed-scale variables. Fragments were the most commonly observed microplastic morphology, with a dominance of gray particles and the polymer polyethylene. The findings of this study can inform management decisions regarding microplastic waste and identify hotspots of microplastic pollution that may benefit from remediation.

1. Introduction

Microplastics are an increasing concern in aquatic environments, capable of entering the food web and potentially endangering human health (Baldwin et al., 2020, Li et al., 2020). Microplastic research first gained

http://dx.doi.org/10.1016/j.scitotenv.2022.155143

^{*} Corresponding author. *E-mail address:* changh@pdx.edu (H. Chang).

traction in the 1970s (Carpenter and Smith, 1972), with studies largely addressing marine environments over the next several decades. Freshwater microplastic pollution is a relatively new field of research, with articles published only within the last ten to fifteen years (Granek et al., 2020; Talbot and Chang, 2022). This research expansion has provided valuable insights into the microplastic cycle and the factors that influence their accumulation and distribution in freshwater bodies. River systems, in particular, are critical transportation pathways, carrying microplastics from inland regions to estuarine and marine environments (Jiang et al., 2019; Zhao et al., 2019). Thus, understanding their presence in freshwater environments can shed light on their abundance in marine waters, which may be greater than previously estimated due to recent evaluations of riverine microplastic flux (Hurley et al., 2018).

Developed and industrial regions have been closely linked with microplastic pollution, in part due to high rates of plastic production and increased littering (Huang et al., 2020, Ma et al., 2021, Mani et al., 2015, Townsend et al., 2019). Positive correlations have also been found between microplastic pollution and percent of impervious cover in watersheds, which greatly serves to enhance plastic transport to aquatic environments (Baldwin et al., 2016). In addition, wastewater treatment plants (WWTPs) are often situated in developed areas, and have been linked with increased microplastic concentrations downstream of effluent outfalls (Estahbanati and Fahrenfeld, 2016; Hoellein et al., 2017). Most treatment processes are not designed to remove tiny plastic particles, and may result in WWTPs serving as important delivery pathways of microplastics to freshwater environments (Mani et al., 2015; McCormick et al., 2016). Additionally, population density has been positively correlated with microplastic concentrations (Battulga et al., 2019; Huang et al., 2020; Kataoka et al., 2019; Ma et al., 2021; Mani et al., 2015; Valine et al., 2020; Yonkos et al., 2014).

Microplastic pollution may also be linked with agricultural regions (Kapp and Yeatman, 2018). Biosolids produced from WWTP processes are commonly used as a fertilizer for crops, yet their application on agricultural lands can result in the introduction of microplastics (particularly microfibers) to these environments (Edo et al., 2020; Leslie et al., 2017). While agricultural soils may serve as a sink for many of these plastic particles (Feng et al., 2020), these soils and the plastics they contain may also be vulnerable to reentering surface water bodies during storms and subsequent runoff events (Kapp and Yeatman, 2018, Peller et al., 2019). Additionally, agricultural regions tend to include the heavy use of plastics (e.g., tarps), which can break down over time and potentially enter freshwater bodies (Campanale et al., 2020; Feng et al., 2020; Grbić et al., 2020; Guerranti et al., 2017).

In addition to variations in spatial distribution, microplastic concentrations vary on a temporal basis as well (Talbot and Chang, 2022), in part due to precipitation and runoff (Cheung et al., 2019; Xia et al., 2020). For instance, many studies report increased microplastic concentrations during the wet season, as land-based microplastics may be introduced to waterways via storm runoff (Eo et al., 2019; Hurley et al., 2018). As such, precipitation may serve to flush microplastics into aquatic environments with subsequent increased microplastic concentrations reported (Hitchcock, 2020; Schmidt et al., 2018; Wong et al., 2020). However, negative relationships have also been observed between precipitation/discharge and microplastic abundance, with the former potentially causing decreased concentrations of the latter due to dilution effects (Barrows et al., 2018; Stanton et al., 2020). These findings indicate the need for additional research conducted on finer temporal scales. Flow rate has also been linked with microplastic concentrations, with gentler hydrodynamics potentially facilitating their accumulation (Kapp and Yeatman, 2018; Mani et al., 2015; Xiong et al., 2019; Watkins et al., 2019). Conversely, higher flow rates in the center of rivers have resulted in observations of decreased microplastic concentrations, with river banks serving as microplastic sinks (Tibbetts et al., 2018).

As research in the field of freshwater microplastics is still in the early stages, much is still unknown regarding their spatial and temporal distributions and links to potential sources. Many studies include a snapshot of

microplastic pollution (i.e., a single sampling session) in freshwater bodies (Di and Wang, 2018; Hoellein et al., 2017; Mao et al., 2020). Few studies have examined variations in microplastic concentrations as a function of seasonality, with even fewer addressing variations observed within the wet season. Differences likely exist between microplastic concentrations in the early versus the late wet season due to factors such as the flush effect and flow dependency (Watkins et al., 2019). Thus, our understanding of the drivers of microplastic abundance would greatly benefit from such a temporal comparison.

Additionally, there are few studies that address microplastic concentrations along a broad urban-rural gradient (Campbell et al., 2017; Campanale et al., 2020b; Lahens et al., 2018). Analyses of this type are particularly critical, as their examination could reveal potential sources and delivery pathways of microplastic pollution. Furthermore, while the presence of other pollutants and contaminants has been well-documented in rivers in the Portland area (Chang et al., 2019; Chen and Chang, 2019; Chen and Chang, 2014; Pratt and Chang, 2012), much remains unclear regarding the degree to which microplastics impact Portland's freshwater bodies (Valine et al., 2020).

This study aims to address these data and knowledge gaps by investigating microplastics in Portland watersheds with varying degrees of development, and by evaluating temporal variability in microplastic concentrations and attributes with different flow regimes. In particular, the objectives of this research are to (i) evaluate how watershed attributes such as land use, arterial road length, and slope influence microplastic concentrations, (ii) evaluate the influence of temporal variability on microplastic concentrations and attributes such as size and color, (iii) evaluate the influence of water velocity and precipitation on microplastic concentrations and loads, and (iv) determine the most common microplastic morphologies (e.g., fiber, fragment, etc.) to evaluate links with potential sources. It is hypothesized that larger size and higher concentrations and loads of microplastics will be found adjacent to developed and agricultural areas as well as in wet season samples, particularly early in the season due to flush effects.

2. Methods

2.1. Study area

Two Portland area watersheds served as the focal points for this study, including the Clackamas River watershed and the Johnson Creek watershed (Fig. 1). These watersheds were selected to assess potential microplastic distributions along an urban-rural gradient in the Portland metropolitan area. Both are comprised of a range of land cover characteristics, thus exposing their waterways to a multitude of anthropogenic activities. The upper reaches of Johnson Creek flow through a continuum of rural and agricultural lands, and the lower reaches are exposed to a much greater degree of development. The Clackamas River also spans an urban-rural gradient, with upper reaches adjacent to forested and mountainous regions and lower reaches located near agricultural lands and varying degrees of development. The Clackamas is a major tributary to the Willamette River and serves as a source of drinking water to 350,000 residents in the Portland metro area (Chen and Chang, 2019). The main soil type present in the study region is silt loam (Natural Resources Conservation Service, 2021).

Samples were collected from 10 study sites, with four located in the Clackamas River watershed and six in the Johnson Creek watershed (Table 1). The majority of sites were selected to coincide with USGS gaging stations, with the intent of using USGS flow data when riverine conditions prevented the collection of such data in situ. There are three exceptions to this, including one site located near the confluence of Rock Creek and the Clackamas River that was selected to further represent potential impacts of developed and residential regions on microplastic pollution. Additionally, one site is located on the North Fork of Deep Creek, a tributary to the Clackamas that is heavily influenced by agricultural activities. Lastly,

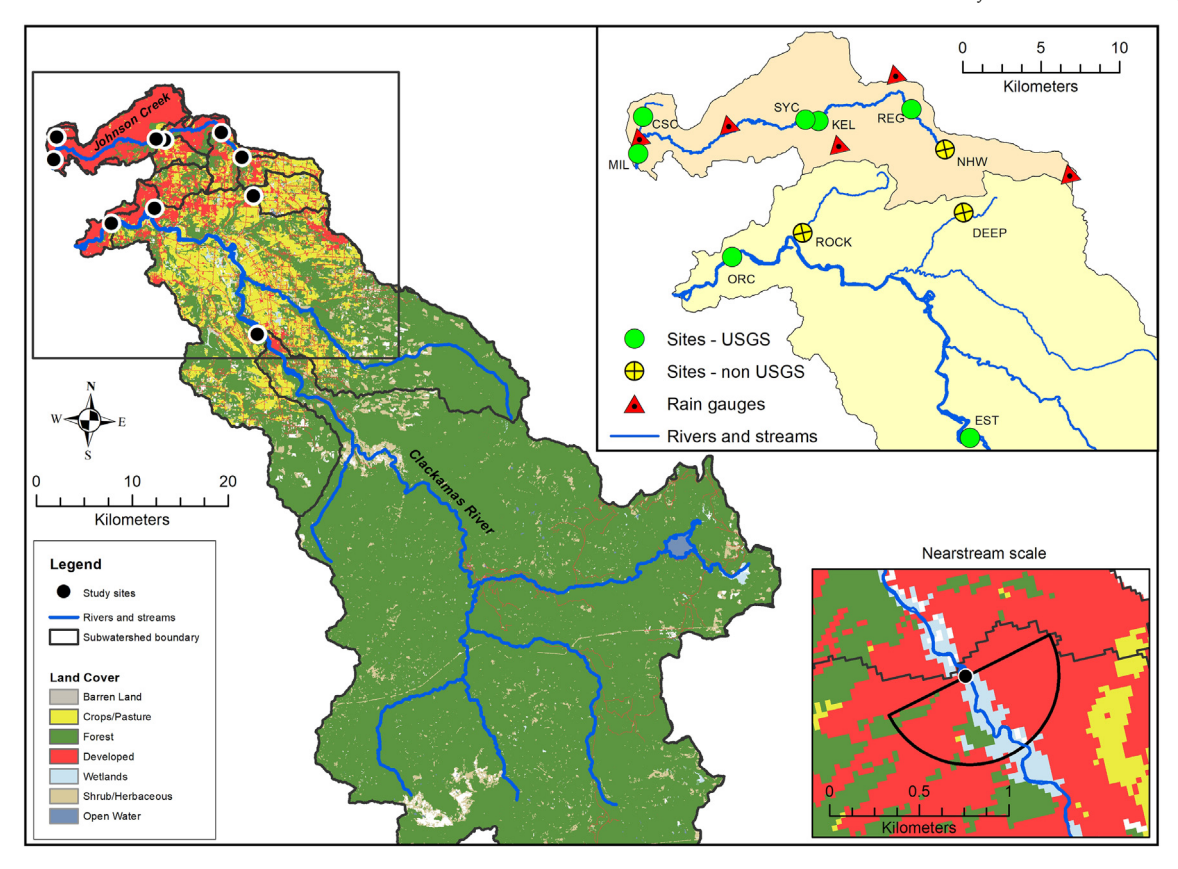


Fig. 1. Map of study area land cover, study sites and rain gauges, at the subwatershed and nearstream scales of analysis.

one site is located near the headwaters of Johnson Creek to further shed light on microplastic sources to the river.

2.2. Data and derivation of explanatory variables

Average flow velocity measurements over 60-second intervals were collected during each sampling session with a Marsh McBirney Flo-Mate flow meter. When river conditions prevented the safe collection of these data (namely the February sampling sessions for the Sycamore and Milwaukie sites), USGS data were downloaded from the National Water Information System (NWIS) database (USGS Water Data for the Nation, 2021) for

Table 1Characteristics of stream monitoring sites used for analysis.

Monitoring sites	USGS gaging number	Drainage area (km²)	Elevation (m)	Dominant land cover (%)
Johnson Creek				
Near headwaters* (NHW)	_		119	Agriculture (50%)
Regner Rd, Gresham (REG)	14,211,400	39.78	91.5	Developed (44%)
Kelley Creek (KEL)	14,211,499	12.15	74.7	Developed (47%)
Sycamore (SYC)	14,211,500	69.41	68.5	Developed (69%)
Milwaukie (MIL)	14,211,550	137.71	6.0	Developed (90%)
Crystal Springs Creek (CSC)	14,211,542	7.90	13.3	Developed (93%)
Clackamas River				
Estacada (EST)	14,210,000	1737.88	87.4	Forest (92%)
Deep Creek* (DEEP)	_		141.0	Agriculture (62%)
Rock Creek* (ROCK)	_		39.0	Developed (43%)
Near Oregon City (ORC)	14,211,010	2434.59	9.0	Forest (58%)

^{*} Not a USGS monitoring site.

stream gauges corresponding with the microplastic sampling locations. In these instances, similar historical discharge/gauge measurements were identified and the corresponding velocity readings were included in the current study. For the Estacada site, 15-minute incremental precipitation data were obtained from the USGS gaging station located on site. Hourly precipitation data were obtained from the City of Portland HYDRA Rainfall Network for the remaining nine sites, and data from the gauges closest in proximity to the study sites were used (particularly if they were located upstream), and are thus estimates of precipitation at the sites (Bureau of Environmental Services, 2021).

Subwatersheds were delineated for each study site using ArcHydro Tools in ArcGIS 10.8.1 (ESRI, 2020), resulting in the creation of distinct, non-overlapping polygons (Mainali and Chang, 2018; Pratt and Chang, 2012). A land cover raster layer of Oregon was downloaded from the National Land Cover Dataset (NLCD) 2019 (Multi-Resolution Land Characteristics Consortium, 2021), and clipped to the subwatershed boundaries. Because the NLCD dataset includes a broad range of land cover categories, they were combined into a single category as appropriate (e.g., deciduous forest, evergreen forest, and mixed forest were combined into a single 'forest' category). Total percentage of each land cover category (agricultural, developed, forest, shrub, and barren) were then derived for each subwatershed by utilizing the zonal histogram tool in ArcGIS. Additionally, subwatershed area was derived for each site.

Nearstream buffer zones were also created in ArcGIS, in which a 500 m upstream buffer was derived for each study site. Mainali and Chang (2018) found that nearstream buffer zones (i.e., a 100 m circular upstream buffer and a 1 km riparian upstream buffer) more fully accounted for processes involved in water quality, with watershed-scale processes being less influential. As the current study included a single nearstream analysis, and as a 1 km upstream buffer would have resulted in overlapping buffer zones across several sites, 500 m was deemed an appropriate upstream buffer

(Fig. 1). Slope was derived in ArcGIS at both scales, in which the zonal statistics by table tool was used to calculate the average slope within each subwatershed and within each nearstream buffer zone (Table 2). In addition, total arterial road length in the nearstream buffer zones for each site was computed using the statistics function in ArcGIS.

2.3. Data collection

2.3.1. Preparatory work

Before collecting samples at the study sites, materials were prepared in the Applied Coastal Ecology (ACE) lab at Portland State University. Quart-sized glass mason jars were rinsed three times with filtered (0.7 μm) deionizied (DI) water, with a layer of aluminum foil present underneath the cap to prevent contamination from the plastic ring present in the cap. Jars were then filled partway with filtered DI water, to be used for rinsing the contents of the cod-end into the sample mason jar. Mason jars were also labeled with appropriate sampling information, including the month, site, and subsample number.

2.3.2. Sample collection

Samples were collected via wading from the center of the stream, where possible. Sites for which this was not possible (namely sites directly along the Clackamas) required a different approach, which involved wading into the river and collecting samples at a standard depth of one meter. Otherwise, water depth at each sampling location was recorded using a meter stick. Where possible, stream width was also measured and recorded using a transect tape. Before beginning sample collection, the plankton net and cod-end were rinsed three times in the river water to prevent cross-contamination from previous sites.

Samples were captured by completely submerging an 80 µm mesh plankton tow net just below the water surface for 15-minute intervals (Valine et al., 2020) and holding it stationary. While excess water flowed directly through the net, microplastic particles and bits of organic debris (most commonly leaves, pine needles, and twigs) were captured in the cod-end that was attached to the tapered end of the plankton net (these larger pieces of organic debris were later rinsed thoroughly into the corresponding sample during processing and then discarded, see Appendix S1). Three replicates were collected per site to examine within-site microplastic variability, and given that within-site microplastic subsamples are not substantially different except for a few August samples (Table S1), these values were subsequently averaged (Campanale et al., 2020b; Valine et al., 2020). A control jar filled with DI water was placed next to the sampling site, and the lid was removed when each sampling session commenced and closed at the completion of sampling to capture airborne microplastics.

At the end of each sampling interval, the net was positioned upright and rinsed down thoroughly with river water to move microplastics down into the cod-end. The cod-end was tapped periodically as necessary to allow for excess water to escape, and the sample was poured into the appropriately labeled mason jar. The cod-end was then rinsed thoroughly with filtered DI water to collect any microplastics that may have been stuck to the sides, and poured into the mason jar. Once the lid was placed over the sample, the lid for the control jar was also replaced. The net and cod-end were then separated and thoroughly rinsed in the river before departing for the

next site. All samples were stored in refrigerators until the commencement of laboratory procedures.

Samples were collected during three sampling sessions to investigate the impacts of temporal variability on microplastic concentrations (Barrows et al., 2018). The first session took place on August 28–30, 2020 and represented microplastic abundances during the dry season and thus without the influence of antecedent precipitation. Only one session was conducted in the dry season, as microplastic concentrations are unlikely to vary significantly throughout summer baseflow conditions. The second sampling session took place on September 24–25, 2020, representing microplastic concentrations in the early wet season when land-based microplastics have been flushed into aquatic environments (Hitchcock, 2020; Kataoka et al., 2019). The last sampling session occurred in the middle of the wet season on February 2–4, 2021, when microplastic concentrations in rivers are potentially more flow-dependent and less impacted by flush effects (Kataoka et al., 2019; Yonkos et al., 2014).

Water volume for each subsampling was computed using the following equation:

$$Volume = A \times T \times V (m/s)$$

Where: A = area of the net opening (m2); V = average velocity of the water (m/s) (Campanale et al., 2020a).

Microplastic concentrations were computed by dividing the total count of each subsample by the water volume sampled, thus standardizing the data (de Carvalho et al., 2021). The microplastic concentrations of each subsample were then averaged at each site during each sampling session, resulting in a single microplastic concentration per site per season. In addition, daily microplastic loads were calculated by multiplying the average microplastic concentration at each site for each sample date by the corresponding daily average discharge (Park et al., 2020) and then multiplying by the total number of seconds in a day (86,400). It is important to note that these calculations were performed only at study sites for which USGS daily average discharge data were available (EST, ORC, REG, KEL, SYC, and MIL).

2.3.3. Sample processing

In preparation for microscope analyses, a series of laboratory procedures were conducted to isolate microplastics on filter papers (Whatman 1820-047 Glass Microfiber Binder Free Filter, 1.6 $\mu m,\, 4.3$ s/100 mL Flow Rate, Grade GF/A, 4.7 cm Diameter) (Valine et al., 2020). Samples were first put through an organic matter digestion step using a 10% potassium hydroxide solution (methods adapted from Baechler et al., 2020), then filtered through a 63 μm sieve, followed by density separation using a hypersaline solution. Lastly, they were vacuum filtered onto filter paper, each of which was stored in a petri dish in a covered cardboard box until microscope analysis with a Leica MZ6 dissecting microscope (12–120 \times magnification). Further details regarding laboratory procedures are given in Appendix S1.

For microscope analyses, stickers showing 12 numbered pie wedges were first affixed to the bottom of each petri dish to aid in both orientation and the tracking of relative locations of plastic particles. Filters were examined using a Leica MZ6 dissecting microscope, and methodologies outlined

Table 2
Variables used in analysis of microplastics in two Portland metro watersheds.

	•	•		
Variable type	Agency source	Data	Derived variable	Original data
Independent	MRLC	National land cover dataset 2019 (30 m)	Agriculture (%)	Pasture, cultivated crops, hay
			Urban (%)	Low, medium, high intensity developed
			Forest (%)	Deciduous, evergreen, mixed
Independent	Oregon Metro	Oregon 30 m DEM	Subwatershed and nearstream slope averages (deg)	Slope (deg)
Independent	Oregon Metro	Streets layer (m)	Total arterial road length in nearstream buffer zones	Arterial road length (m)
Independent	USGS	Streamflow (15-60 min intervals)	M/s at time of sampling	Discharge (cms)
Independent	HYDRA	Precipitation (60-min intervals)	24- and 72-h antecedent precip (mm)	Precipitation amount (mm)
	USGS	Precipitation (15-min intervals)		
Dependent	This study	Microplastic concentration	Count per volume (particle/m³)	Total microplastic count and water volume sampled

in the Guide to Microplastic Identification (Marine & Environmental Research Institute, nd) were followed to aid in the distinction between microplastics and biotic material. For instance, particles showing cellular structure were excluded, along with fiber-like particles characterized by tapering. Additionally, particles that broke apart upon manipulation with a metal probe were also excluded. In these instances, the particle in question was assumed to be biological or non-plastic in nature.

Filter inspection began in the upper left section and continued in a straight line across the filter paper, with the aforementioned metal probe used to explore and prod particles to determine flexibility. Inspection of the row below commenced at the right side of the paper and continued to the left, and this horizontal pattern was repeated for each row of the filter paper. When a suspected microplastic was identified, information regarding type (fiber, fragment, film, foam, tire wear particle), color, maximum length, and magnification level were recorded on a datasheet. In addition, photographs were taken of each suspected microplastic and saved to a google drive for future reference and use. A control petri dish with a clean filter was placed next to the scope to assess contamination from airborne particles, and was evaluated for microplastics between each scoped study sample (Valine et al., 2020).

2.3.4. Quality control

Given the mesh size of the plankton tow net, the study focused on particles greater than 80 μm , but some particles between 63 and 80 μm were retained due to the use of a $63 \mu m$ sieve during processing; we include all microplastics >63 μm in our dataset. To minimize the risk of contamination, orange cotton jumpsuits were worn during sample collection, lab procedures, and microscope analyses. In addition, nitrile gloves were worn during all lab procedures and analyses. Any orange particles noted in samples were excluded from the final microplastic counts. Both field and laboratory controls were employed to evaluate background microplastic contamination in these environments (Brander et al., 2020). To address potential contamination during laboratory processing, lab controls comprised of 270 mL of filtered DI water underwent the same digestion procedures as field samples, with one control digested with each batch of field samples. Lab controls were also employed during density separation procedures to capture any airborne microplastics. To address contamination during sample collection, a field control jar with filtered DI water was present at each site for each sampling session, with the lid of the control open only during active sample collection.

2.3.5. Subsampling for analytical confirmation

A subset of particles was sent to the Ecotox and Environmental Stress Lab at Oregon State University for micro-Fourier transform infrared ($\mu FTIR$) spectroscopy analysis to identify specific polymers and validate total counts (Baechler et al., 2020; Wang et al., 2020). As part of the selection process, samples were first randomized, as were the 12 sections of each petri dish. To additionally ensure that particles were randomly selected, the authors agreed pre-microscopy to select the third observed microplastic within a specified section for $\mu FTIR$ analysis. One hundred and one particles from field samples were selected by this randomized process, and an additional five were specifically selected to examine particles of interest. In addition, ten particles from controls were included for analysis.

It is important to note that tire wear particles are difficult to identify using μ FTIR spectroscopy, and are more reliably confirmed through methods such as pyrolysis gas chromatography (Primpke et al., 2020; Werbowski et al., 2021). For this reason, the authors placed a cap on the total number of TWPs that were submitted for μ FTIR analysis.

2.3.6. μFTIR analysis

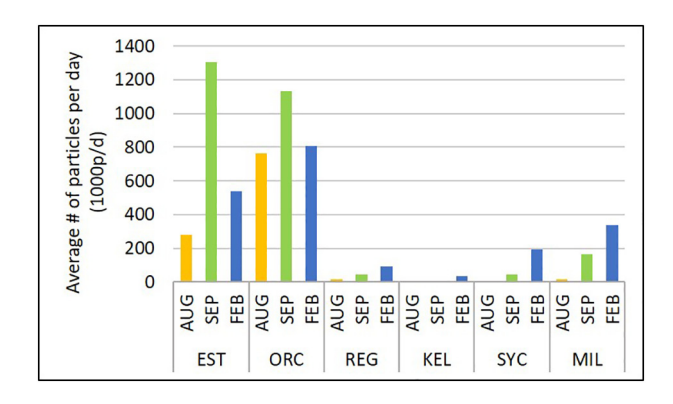
Particles selected for $\mu FTIR$ represented approximately 10% of the total suspected microplastics (Baechler et al., 2020; Harris et al., 2022. The proportion of particles analyzed was based on a combination of variability in particle morphologies found in our samples and funds available for analysis. We are confident that the particles analyzed are representative of the entire sample, and based our rationale for particle

subsampling and analysis on Brander et al. (2020) and Cowger et al. (2021). μ FTIR methodologies were similar to those detailed by Harris et al., 2022. Briefly, under a laminar-flow hood, particles were picked from filters and stored between glass microscope slides. Each particle was confirmed under a Leica EZ4E to match with images from PSU. Samples were placed on a gold-plated slide and subsequently reflectance was measured using a Thermo Electron iN5 μ FTIR (Thermo Fisher Scientific), followed by insertion of a germanium tip probe (ATIR) approximately 1–2 μ m into the material's surface. A math match cut-off of 70 or greater was used for all samples, with all spectra being confirmed and smoothed via Open Specy (Cowger et al., 2021) and crosschecked with Omnic software per methods adapted from Baechler et al. (2020) and Harris et al., 2022 (Fig. S1).

2.3.7. Statistical analysis

Statistical analyses were conducted in R, version 1.4.1717 (R Core Team, 2021), using the corrplot (v0.90; Wei and Simko, 2021), the FSA (v0.9.1; Ogle et al., 2021), the lattice (Sarkar, 2008), the ggbiplot (v0.55; Vu, 2011), and the plyr (Wickham, 2011) packages. Because assumptions of normality and equal variance were not met, nonparametric statistics were used to assess potential relationships between explanatory variables and microplastic concentrations. To determine potential influences of temporal variability, a Kruskal-Wallis rank sum test was run to compare average microplastic size, concentrations, and morphologies across the three sampling sessions. To assess whether differences may exist between sites, the ten study sites were first divided into two groups based on land use. At the subwatershed scale, the Developed group was comprised of sites with subwatersheds characterized by greater than 40% developed land (CSC, MIL, SYC, ROCK, REG, and KEL), with the Mixed/Rural group comprised of the remainder (EST, ORC, DEEP, and NHW). At the nearstream scale, the Developed group was comprised of sites with nearstream regions characterized by greater than 60% developed land (DEEP, CSC, NHW, REG, SYC, and MIL), with the Mixed/Rural group comprised of the remainder (EST, ROCK, ORC, and KEL). These groups were then further subdivided based on sampling session, for a total of six groups. Kruskal-Wallis rank sum tests were then run to compare average microplastic concentrations based on these site categories as a function of sampling session, and to compare microplastic morphologies and size classes across the sampling sessions.

Spearman's rank correlation was used to compare average microplastic concentrations with spatial and temporal predictor variables. Spatial variables included subwatershed area, total arterial road length, land use, and slope (the latter two included both subwatershed and nearstream scales, see Table S2 for correlations between spatial explanatory variables). Temporal variables included average water velocity during each sampling session, 24-hour antecedent rainfall, and 72-hour antecedent rainfall.



 ${\bf Fig.~2.}$ Daily microplastic loads at six USGS gaging stations across the three sampling sessions.

3. Results

3.1. Characteristics of microplastics

Microplastics were found at all sites, with a total of 1009 particles observed across the 90 field samples. An additional 490 particles were found across the 30 field and 53 lab controls (Table S3A, Table S3B). Scope controls revealed minimal aerial deposition of microplastics, with a fiber typically noted every few field samples (Table S3C). Four microplastic morphologies were observed in field samples, including fragments (n = 505, 50.1%), fibers (n = 173, 17.1%), films (n = 71, 7%), and foams (n = 23, 2.3%) (Fig. 3). Additionally, 237 suspected tire wear particles (23.5%) were observed in field samples. Throughout the visual identification process, suspected TWPs displayed a unique set of characteristics that set them apart from other morphologies. More specifically, their appearance was generally bumpy/rough and rubbery in nature, typically cylindrical in shape, black in color, and quite pliable (Klasios et al., 2021; Parker et al., 2020).

Microplastics fell into one of nine color categories: gray (n = 367, 36.4%), black (n = 313, 31%), blue (n = 174, 17.2%), white/clear (n = 174, 17.2%) 66, 6.5%), pink (n = 39, n = 3.9%), green (n = 17, 1.7%), red (n = 17, 1.7%), r 1.7%, purple (n = 10, 1%), and yellow (n = 6, 0.6%) (Fig. 4). Microplastics were also divided into five size classes (Campanale et al., 2020b; Cheung et al., 2019; Huang et al., 2020): 63-100 μ m (n = 17, 1.7%), 101-500 μ m $(n = 402, 39.8\%), 501-1000 \, \mu \text{m} (n = 318, 31.5\%), 1001-2000 \, \mu \text{m} (n = 318, 31.5\%)$ 184, 18.2%), and 2001-5000 μ m (n = 88, 8.7%) (Fig. 5a). Thus, microplastics less than 0.5 mm in length comprised over 40% of the observed plastics, with nearly three-fourths of particles measuring less than 1 mm. µFTIR analyses of the 116 submitted particles identified a total of nine polymer types: polyethylene (PE), polypropylene (PP), polystyrene (PS), polyethylene terephthalate (PET), cellulose, cellophane, ethylene vinyl acetate, polyvinyl acrylonitrile, and styrene butadiene (likely tire particles). Dominant polymers in field samples included PE (30%), PP (27%), cellulose (17%), and PET (9%) (Fig. 6): See Fig. S1 for example spectra of PE, PP, PET, cellulose, and styrene butadiene and Fig. S2 for typical polymers.) For Fig. 6, it is important to note that the authors included very few TWPs in µFTIR analyses, due to the difficulty in identifying them via this method of spectroscopy. For this reason, TWPs appear to comprise a

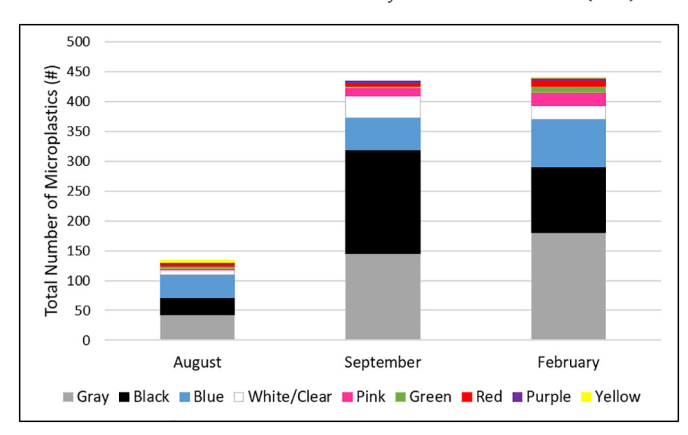


Fig. 4. Color composition of microplastics across three sampling sessions.

very small percentage of the observed polymers. Additionally, over half of the analyzed particles were fragments, with approximately one-quarter in the 101-500 mm size class. Every particle evaluated by $\mu FTIR$ was either synthetic or anthropogenically impacted (modified by humans such as cellulose, wool clothing; per Harris et al., 2022).

3.2. Differences across sites and sampling sessions

While the highest microplastic abundances for each sampling session were observed at the MIL site (August: n=30; September: n=207; February: n=135), the KEL site had the highest concentration for August (37.73 p/m³), the MIL site had the highest concentration for September (1.76 p/m³), and the NHW site had the highest concentration for February (0.89 p/m³). Calculations of daily microplastic loads at six study sites showed the highest loads at the EST and ORC sites, particularly during the September sampling session (Fig. 2). The abundance of microplastics in the 101-500 μ m size class differed significantly between August and September (Kruskal-Wallis, H(2) = 9.2408, p < 0.05), with these particles dominating in the September sampling session. In addition, the abundance of microplastics in the 2001-5000 μ m size class differed significantly between September and

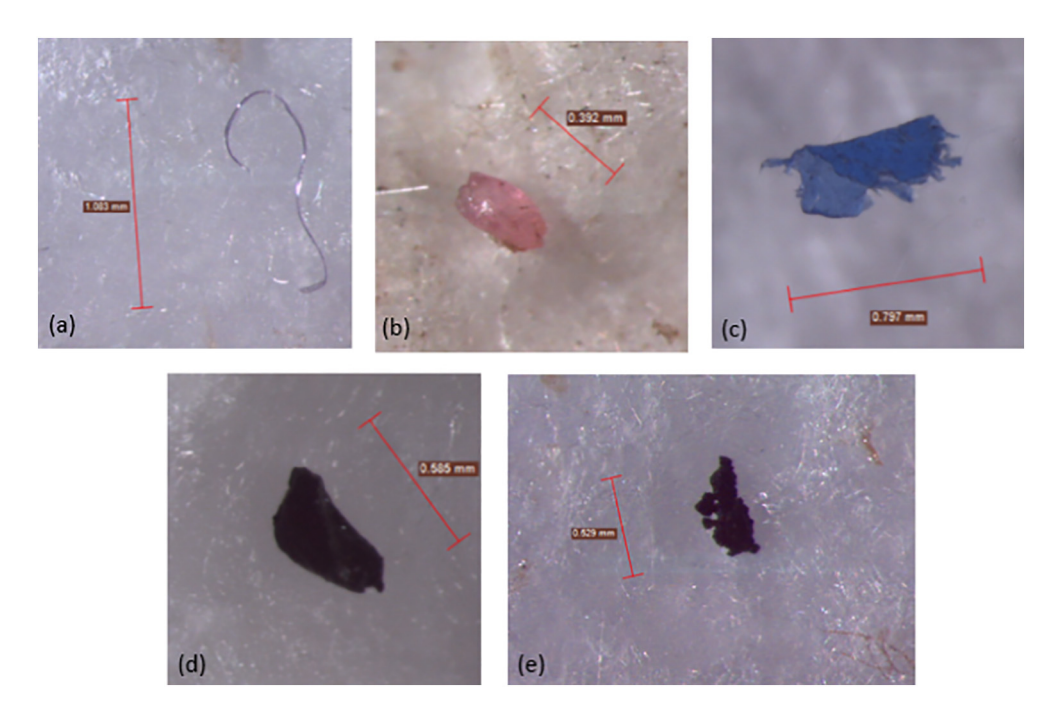
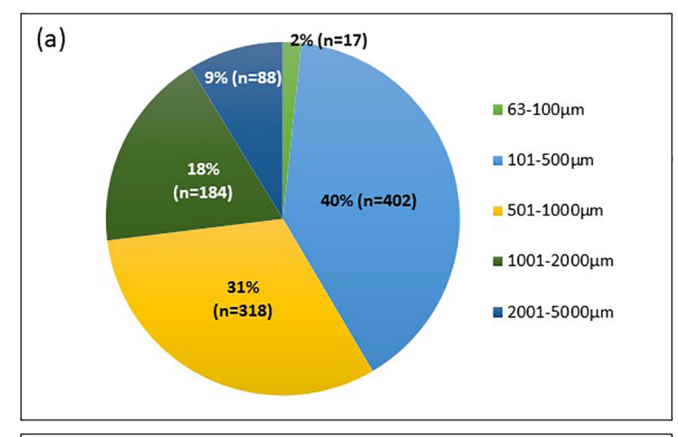


Fig. 3. Examples of microplastics found in Johnson Creek and the Clackamas River, Oregon USA: (a) purple fiber; (b) pink fragment; (c) blue film; (d) black foam; and (e) black tire wear particle.



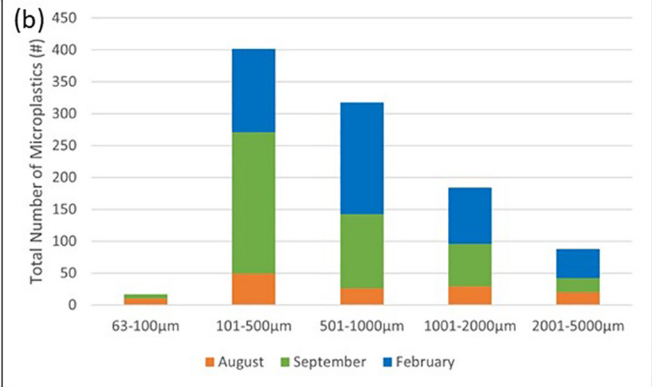


Fig. 5. (a) Size composition of microplastics; and (b) distribution of size classes across the three sampling sessions.

February (Kruskal-Wallis, H(2) = 6.0872, p < 0.05), with higher abundances observed in February (Fig. 5b). Differences were also found between the average microplastic concentrations observed during the three sampling sessions (Kruskal-Wallis, H(2) = 6.1342, p < 0.05). Results of a post-hoc Dunn test were inconclusive due to low statistical power, but an examination of boxplots indicated differences between August and February. More specifically, average microplastic concentrations were highest in August (3.24 \pm

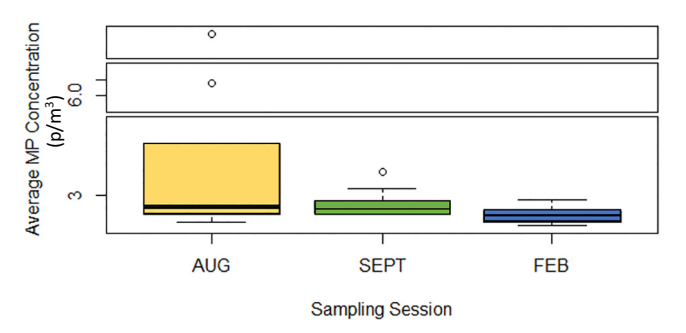


Fig. 7. Average microplastic concentrations in Johnson Creek and the Clackamas River, Oregon, USA during three sampling sessions in 2020 and 2021.

1.84 p/m³) and lowest in February (0.365 \pm 0.076 p/m³) (Fig. 7). Microplastic concentrations ranged from 0.19–18.86 p/m³ in August, 0.43–1.69 p/m³ in September, and 0.09–0.85 p/m³ in February (Fig. 8).

At the subwatershed scale, no differences in average microplastic concentrations were observed between the Developed and Mixed/Rural groups (Kruskal-Wallis, H(5) = 8.2333, p > 0.1). A difference was observed at the nearstream scale (Kruskal-Wallis, H(5) = 11.852, p < 0.05), with a posthoc test revealing a significant difference between the August sampling at Developed sites (higher concentrations) and the February sampling of Mixed/Rural sites (lower concentrations) (Dunn's test, p < 0.05). Thus, despite sampling across multiple land use types and sampling sessions, there only existed a difference between August and February, with no differences between the Developed and Mixed/Rural groups observed during any single sampling session.

Proportions of the microplastic morphologies appeared to vary across the sampling sites and sessions (Fig. 9). Of particular note is the relatively low proportion of fibers present at the EST and ORC sites in the dry season, which then became the dominant morphology for both sites in the mid-wet season. Conversely, three Johnson Creek sites (REG, KEL, and SYC) demonstrated the opposite trend, in which fibers were the dominant morphology in the dry season and then dropped to much lower proportions in the mid-wet season. Several morphologies showed statistically significant differences across sampling sessions, including fiber concentrations (Kruskal-Wallis, H(2) = 8.0852, p < 0.05), film concentrations (Kruskal-Wallis, H(2) = 6.1258, p < 0.05), and tire wear particle (TWP) concentrations (Kruskal-Wallis, H(2) = 8.6157, p < 0.05). A post-hoc Dunn test

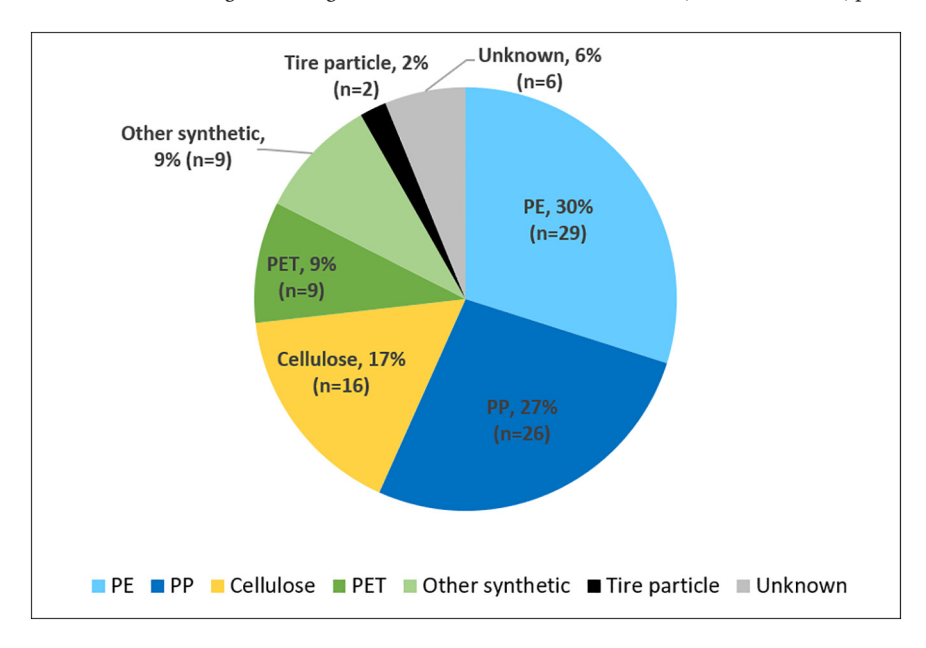
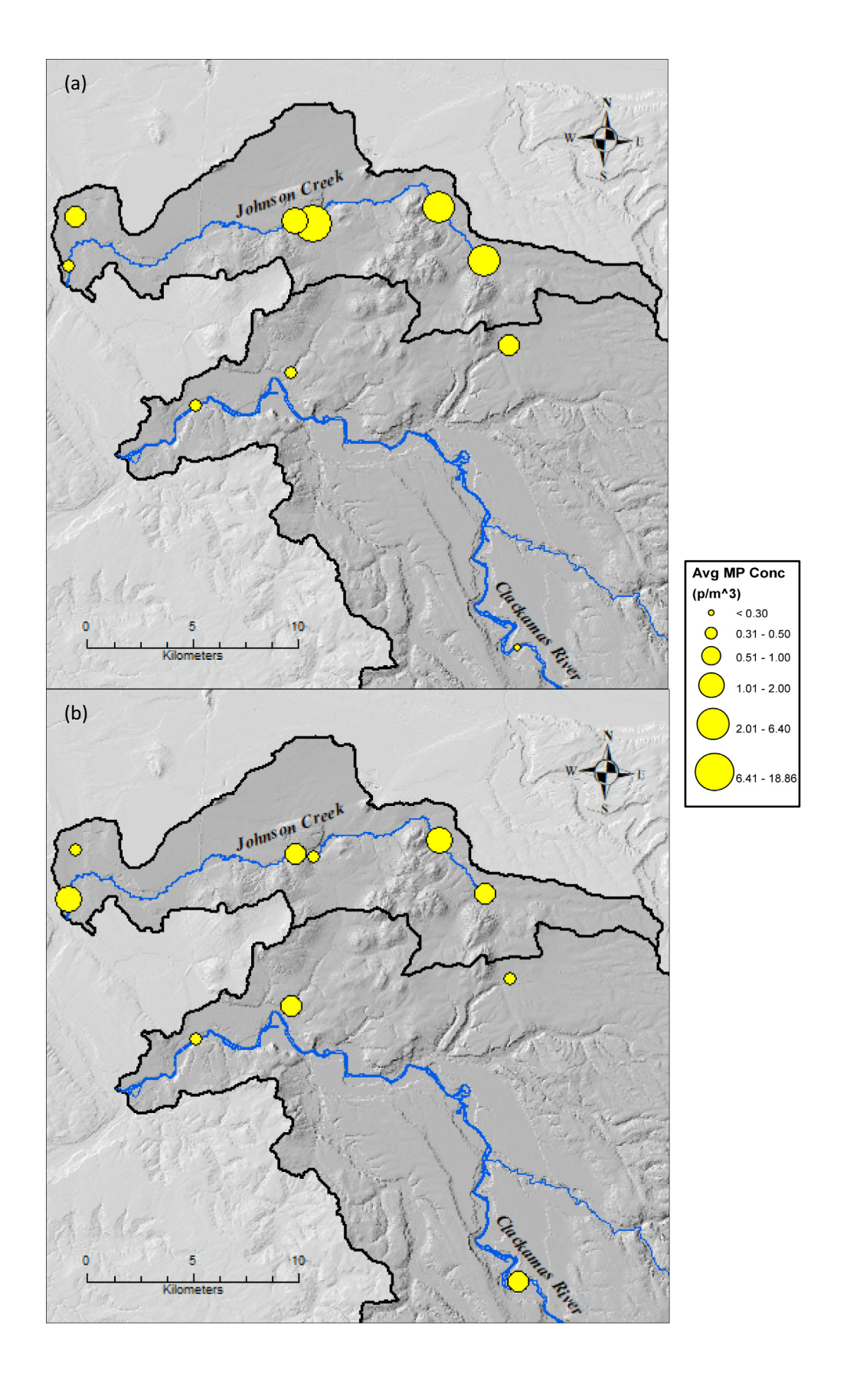


Fig. 6. Polymer composition of microplastics evaluated by μ FTIR spectroscopy. Note: only one PE particle was characterized as high-density PE, the rest were comprised of low-density PE.



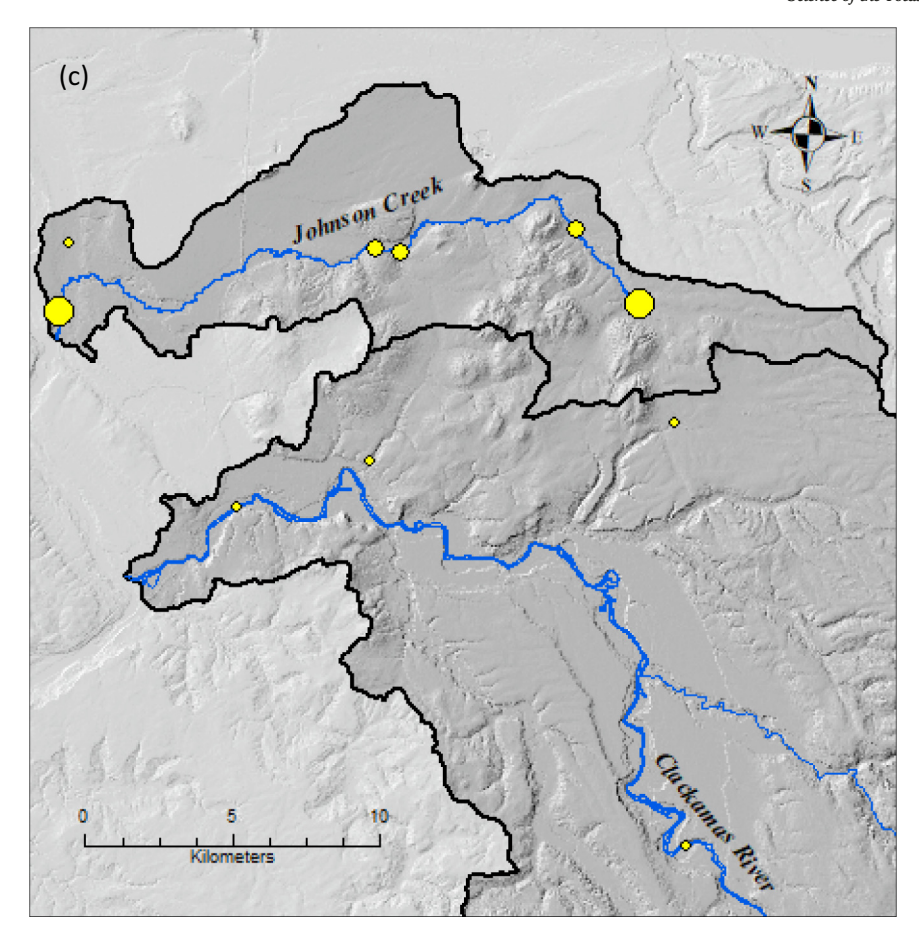


Fig. 8. Microplastic concentrations at each monitoring site in Johnson Creek and the Clackamas River, Oregon, USA during the sampling sessions of (a) August 2020 (b) September 2020 and (c) February 2021.

revealed that August TWP concentrations differed significantly from September concentrations (p < 0.05), with higher concentrations observed in September. August fiber and film concentrations differed from February concentrations (p < 0.05), with higher concentrations for both morphologies observed in August.

3.3. Correlations between microplastic concentrations and explanatory variables

Average microplastic concentrations for each of the three sampling sessions were correlated with several spatial and temporal variables (Tables 3 and 4, respectively). Only two correlations were significant with regard to temporal factors, with higher microplastic concentrations in August linked with lower average water velocities (r=-0.854, p<0.05) and higher microplastic concentrations in February coinciding with increased rainfall in the 24 h preceding sample collection (r=0.638, p<0.05). At the spatial level, both September and February microplastic concentrations were lower in predominantly agricultural lands at the nearstream scale (r=-0.721, p<0.05 and r=-0.673, p<0.05, respectively). Sites with greater proportions of shrub land had lower microplastic concentrations in February at the subwatershed scale (r=-0.721, p<0.05), and greater subwatershed area was linked with lower microplastic concentrations in August. (r=-0.673, p<0.05).

4. Discussion

4.1. Microplastic characteristics

Fragments were the dominant morphology observed in this study, similar to findings from previous studies (Bertoldi et al., 2021; Mai et al., 2021; Tibbetts et al., 2018). Fibers have also been noted as a dominant

morphology (Belen Alfonso et al., 2020; Chen et al., 2020; Feng et al., 2020; Hu et al., 2020), though they were the second most common morphology at our study sites. The dominance of gray particles in the current study is unusual (with the bulk of gray particles analyzed by $\mu FTIR$ being PE, followed closely by PP), as the literature shows that dominant colors typically include blue (Barrows et al., 2018; Dris et al., 2018; Miller et al., 2017; Strady et al., 2020), clear/white (Baldwin et al., 2020; Di and Wang, 2018; Han et al., 2020; Huang et al., 2020), and black (Guerranti et al., 2017; Qin et al., 2020; Sang et al., 2021). Greater proportions of clear/white plastics in particular may result from processes such as photodegradation (Fan et al., 2019). We suspect that the dominance of gray particles in the current study is associated with particular industry sources, based on the proximity of certain industries to our sample sites (e.g., a warehousing and transportation company, an industrial refrigeration company).

The dominance of plastic particles under 1 mm in length is consistent with previous research (Bertoldi et al., 2021; Bujaczek et al., 2021; Sang et al., 2021; Wang et al., 2021). Indeed, an inverse relationship between microplastic size and concentration is a common finding in freshwater microplastic research (Battulga et al., 2019; Fan et al., 2019; Schmidt et al., 2018). Additionally, the abundance of microplastics in different size classes can vary across time. More specifically, a significantly greater abundance of particles in the largest size class (2001-5000 μm) in February than in September is an interesting finding, and may indicate lower rates of degradation during the rainy season (Amrutha and Warrier, 2020). de Carvalho et al. (2021) reported a dominance in smaller size classes of microplastics during periods of low flows. Thus, the significantly greater abundance of small particles (101-500 μm) in September as opposed to August in the current study is also interesting, as the August sampling session was conducted during low flow conditions.

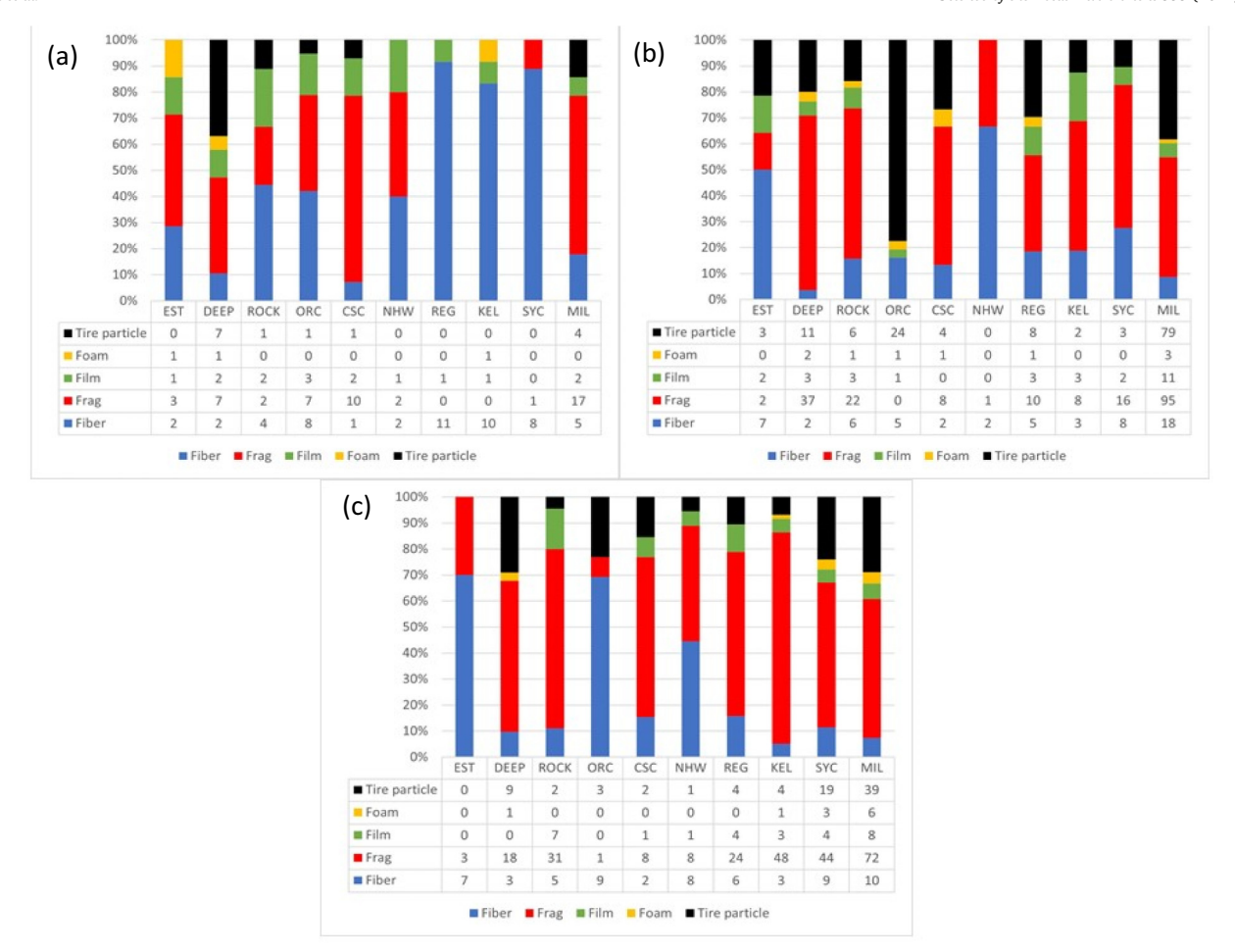


Fig. 9. Proportion of microplastic morphologies observed by site and by sampling session: (a) August 2020 (b) September 2020 and (c) February 2021.

Only one other study has evaluated microplastic concentrations in Oregon's freshwater bodies (Valine et al., 2020), including dry season sampling along the Willamette River (of which both Johnson Creek and the Clackamas River are tributaries) and adjacent to the Oregon Museum of Science and Industry (OMSI) in Portland. Valine et al. (2020) noted a dominance of fibers, reporting an average concentration of 3.19 fibers/m³ at the OMSI site. In comparison, dry season sampling in the current study showed two sites along Johnson Creek exceeding the average concentration reported at OMSI (KEL - 18.9 p/m^3 ; REG - 6.4 p/m^3), with the remaining eight sites showing average concentrations of less than 2.5 p/m^3 during dry season sampling.

4.2. Temporal variability and hydrodynamic variables

Microplastics were identified at all sites throughout all sampling sessions, and an investigation of the literature shows similar findings of microplastic ubiquity (Ballent et al., 2016; Constant et al., 2020; Shruti

et al., 2019; Yin et al., 2020). Microplastic pollution varied temporally, with significantly higher concentrations observed during August (dry season) than during February (mid-wet season). It was expected that higher concentrations would be found during the early wet season than during the dry season due to first flush effects, yet the data did not support this hypothesis. While some studies find higher microplastic concentrations in the wet season (Eo et al., 2019, He et al., 2020), others have found that microplastics dominate in dry season samples (de Carvalho et al., 2021; Fan et al., 2021). This is potentially due to increased precipitation and runoff associated with the wet season resulting in dilution effects and lower observed microplastic concentrations (Fan et al., 2019; Stanton et al., 2020; Wu et al., 2020). While microplastic concentrations in the current study were negatively correlated with average flow rates in August (dry season), no correlations were observed between flow and concentrations in September and February (wet season).

There was little evidence that precipitation amount influenced microplastics at the study sites, similar to several previous studies showing

Table 3Correlations between average microplastic concentrations and spatial factors.

		Area	Slope	Road density	Barren	Crops	Dev	Forest	Shrub
Aug	SWS	-0.673*	-0.321		-0.532	0.261	0.455	-0.358	-0.479
	Near		0.042	0.278	-0.337	-0.491	0.455	-0.274	-0.560
Sept	SWS	0.127	0.115		-0.625	-0.091	0.236	-0.127	-0.527
	Near		-0.212	0.127	0.078	-0.721*	0.297	-0.085	0.143
Feb	SWS	-0.430	-0.370		-0.607	0.152	0.564	-0.515	-0.721*
	Near		-0.285	0.491	-0.017	-0.673*	0.564	-0.432	-0.198

^{*} Significant at the 0.05 level; SWS = Subwatershed scale.

Table 4Correlations between average microplastic concentrations and temporal factors.

	Velocity (m/s)	24P (mm)	72P (mm)
August	-0.854*	-	-
September	-0.382	0.309	-0.486
February	-0.212	0.638*	-0.006

24P = 24-hour antecedent precipitation.

72P = 72-hour antecedent precipitation.

no relationship between the two (e.g., Constant et al., 2020; de Carvalho et al., 2021). There was a positive correlation between February microplastic concentrations and 24-hour antecedent precipitation, but the vast majority of precipitation values were estimates, with the closest HYDRA rain gauge at times located several miles away from a particular study site. As a result, data from a particular gauge were at times used for more than one site, a clear study limitation and potentially the reason for a difference between September and February.

In addition, localized rain events in September may have influenced the differences observed between early and mid-wet season antecedent precipitation and microplastic concentrations. These microstorms may have resulted in HYDRA rain gauges not reflecting accurate precipitation amounts at study sites in September. However, these gauges may have reflected more representative conditions in February due to widespread, less localized rain events. As such, precipitation may indeed be an important driver of microplastic concentrations in the study region, but the September sampling session may not have captured this effect. To ensure a clearer picture of potential relationships between precipitation and microplastics, obtaining precipitation data on a finer spatial scale with gauges located within very close proximity to study sites is ideal.

Our examination of microplastic loads at six of the study sites showed that the dry season sampling (August) consistently had the lowest microplastic loads. Conversely, the highest microplastic loads were present in the wet season, with two sites in the Clackamas River having the highest loads during the early wet season (September) and four in Johnson Creek having the highest loads during the mid-wet season (February). This dominance of wet season microplastic loads is consistent with previous research (e.g., Eo et al., 2019).

It is also important to note that the timing of data collection may be critical in evaluating the influence of precipitation. As previously noted, microplastic concentrations can vary drastically over very short periods of time as a function of hydroclimatic variables (Xia et al., 2020), even over the course of several hours (Cheung et al., 2019). Wet season sampling for the current study was conducted over a period of two or three days, due to the limited number of researchers involved in data collection. If multiple collection teams had been available to complete each wet season sampling event in a standardized amount of time and within a single day, this could have contributed to a clearer analysis regarding the impacts of precipitation on microplastic concentrations.

4.3. Watershed attributes

Few spatial variables were found to have significant relationships with microplastic concentrations, for either the subwatershed scale or the nearstream scale. Of important interest, however, were negative correlations between September and February microplastic concentrations and proportion of agricultural lands in the nearstream zones. This indicates that fewer microplastics were found in regions where the immediate upstream area was characterized by a greater degree of croplands, even during wet season periods when runoff is most likely to introduce plastic particles to freshwater bodies. The degradation of plastics used for agricultural purposes thus may not result in the flushing of substantial amounts of microplastics into nearby freshwater bodies; these microplastics may instead remain trapped in permeable agricultural soils (Feng et al., 2020).

Very few studies to date have evaluated microplastics in soils, and additional research is needed to shed further light on the microplastic cycle in both agricultural regions and other land use categories (Amrutha and Warrier, 2020; Feng et al., 2020).

Only one significant relationship was observed at the subwatershed scale, and included a negative correlation between February microplastic concentrations and proportion of shrub land. It is thus possible that nearstream analyses may shed more light when determining relationships between microplastic pollution and potential explanatory factors. Microplastics likely share delivery pathways with other contaminants and nutrients that threaten water quality (Mishell Donoso and Rios-Touma, 2020; Sarkar et al., 2019; Zhou et al., 2020), and as previously noted, recent water quality modeling research has highlighted the importance of nearstream as opposed to watershed-scale processes (Mainali and Chang, 2018). Similar sentiments were expressed by Barrows et al. (2018), whose analyses at the subwatershed scale spurred the belief that more localized analyses (e.g., on specific point sources) may be more useful in understanding the role of potential explanatory factors. A similar emphasis on specific sources of microplastics addressed at local scales was noted by Dikareva and Simon (2019).

While total microplastic counts were highest at the Milwaukie site, which is characterized by a high proportion of developed land cover, an unexpected finding was the lack of a correlation between microplastic concentrations and developed land, at either the subwatershed or nearstream scales. As previously mentioned, the two watersheds included in this study represent a range of land covers, yet it is possible that the selected sites may not represent the full urban-rural gradient, thus clouding potential relationships. For instance, many of the sites were located in mostly developed regions. Perhaps the incorporation of a greater number of study sites spanning a broader range of the gradient may reveal more specific results (Belen Alfonso et al., 2020; Dikareva and Simon, 2019), and this may also be the case with other watershed attributes such as slope. Additionally, as the net was submerged just under the surface of the water to ensure that water volume could be calculated, it is possible that some microplastics on the surface circumvented the net. Lastly, it is important to note that factors not evaluated by the current study (e.g., various microscale processes, sediment resuspension) may have exerted an influence on observed microplastic concentrations. Evaluating microplastic concentrations in sediment samples would have provided further insight regarding influential factors as well as a more comprehensive picture of the microplastic cycle at the monitoring sites.

4.4. Potential sources

Broad links can be made with regard to observed microplastic morphologies and potential sources. As previously mentioned, fragments were the dominant observed morphology, indicating that the breakdown of larger pieces of plastic and litter may be a critical source of microplastics in Portland's freshwater bodies. Fibers were also common, indicating that factors such as washing machine effluent (e.g., in residential regions surrounding the Regner and Kelley Creek sites) or recreational activities (e.g., at sites characterized by a high degree of water activity such as the Estacada and Near Oregon City sites) may play a role in microplastic pollution as well. Additionally, given that the September sampling session showed significantly higher tire wear particle concentrations than the August sampling session, it is likely that these particles accumulated on land during the dry period and were flushed into nearby waterways during the first wet season storm event. The influx of tire wear particles in the early wet season is particularly alarming, as recent research has highlighted the severe threat they pose to salmon (Tian et al., 2021).

The identification of specific polymer types can also shed light on potential sources of microplastic pollution. Polyethylene (PE) was the most commonly observed polymer, which is consistent with previous findings (Fan et al., 2019; Xiong et al., 2019). In particular, PE particles were composed of two sub-polymers with very different applications. Of the 116 particles assessed by $\mu FTIR$ spectroscopy,

^{*} Significant at the 0.05 level.

low-density polyethylene (LDPE) particles were found at all but two of the study sites. These plastics are typically found in thin plastic bags, such as those used in grocery stores (Mishra et al., 2021). In contrast, only one high-density polyethylene (HDPE) particle was reported, and it was observed at the Milwaukie site. As HDPE particles are commonly used in construction activities and PVC pipes (Mishra et al., 2021), its presence at the more industrial Milwaukie site is unsurprising. Polypropylene (PP) was very common as well, and is often found in a variety of packaging materials as well as in synthetic clothing (Mishra et al., 2021). Of the samples that underwent $\mu FTIR$ analyses, PP particles were found at all but two of the sites, underscoring their ubiquity.

4.5. Conservative estimates of microplastics

The observed microplastic concentrations in this study are likely conservative, which may be due to several factors. For instance, the use of a hypersaline solution during density separation does not result in the flotation of 100% of plastic particles, as higher density plastics in particular often remain trapped with sediment (Mishra et al., 2021). Therefore, the vacuum filtration step may have missed microplastics that remained at the bottom of the sample jars (Di and Wang, 2018; Valine et al., 2020), thus resulting in a subset being isolated on the filter paper for microscope analysis. Similarly, the fact that sampling was conducted just below the surfact of the water likely resulted in the underrepresentation of high-density particles such as TWPs, many of which may reside at lower depths in the water column or in benthic sediment (Wik and Dave, 2009).

Additionally, while microplastics in the smallest size class (63-80 $\mu m)$ were retained, this class is likely vastly underrepresented due to the use of an 80 μm mesh net during sample collection. The current study also included the use of glass microfiber binder free filters, which are white in color. While the current study identified some white microplastic particles under the microscope, it is likely that others were missed due to the difficulty in identifying these particles against a white background. The inclusion of clear polycarbonate filters in future studies may facilitate the identification of white microplastics.

5. Conclusion

This study showed that microplastic concentrations in the Portland metropolitan area may be influenced by certain hydroclimatic variables and subwatershed characteristics. In the dry season, lower flow rates appeared to facilitate the accumulation of microplastics, with concentrations also potentially influenced by antecedent rainfall in the mid-wet season. Additionally, microplastic concentrations may be influenced more strongly by nearstream as opposed to subwatershed factors, particularly with regard to adjacent agricultural lands. Fragments were dominant in both watersheds, likely due to the breakdown of larger pieces of plastic. Gray particles were particularly common, and the 101-500 μm size class of microplastics was the most highly represented. Higher concentrations of tire wear particles in the wet season suggest a flushing effect.

The findings of this study further our knowledge of riverine microplastic pollution in the Portland metro area and contribute to our understanding of potential sources of microplastics in freshwater environments. This information is beneficial to local officials and agencies in Portland, who are increasingly interested in knowing the potential sources and pathways of microplastics in their water bodies. Armed with such knowledge, they may be better equipped to enact policies that result in decreased concentrations of microplastics reaching aquatic environments. In addition, the findings of the research can identify hotspots of microplastic pollution that may benefit from remediation, and can potentially assist in projections of microplastic concentrations in other locations with similar characteristics, for which no microplastics data have yet been collected.

CRediT authorship contribution statement

Rebecca Talbot: Conceptualization, Data curation, Methodology, Laboratory analysis, Writing - original draft preparation.

Elise Grank: Conceptualization, Methodology, Supervision, Writing – Review & editing.

Heejun Chang: Conceptualization, Methodology, Supervision, Writing – Review & editing.

Rosemary Wood: Data curation, Methodology, Laboratory analysis. Susanne Brander: Laboratory Analysis, Methodology, Writing – Review & editing.

Declaration of competing interest

The authors declare that they have no known competing financial interests or personal relationships that could have appeared to influence the work reported in this paper.

Acknowledgements

This research was supported by a Faculty Enhancement Grant at Portland State University and National Science Foundation (CBET 2115447 & SMB 1935028). Additional supports were provided by the City of Gresham, City of Portland, Clackamas River Water Providers, East Multnomah County Soil and Water District, and Sigma Xi. We acknowledge and thank Emily Pedersen in the Brander laboratory for conducting FTIR analyses on samples for this study. We appreciate three anonymous reviewers whose comments helped clarify many points of the article.

Appendix A. Supplementary data

Supplementary data to this article can be found online at https://doi.org/10.1016/j.scitotenv.2022.155143.

References

- Amrutha, K., Warrier, A.K., 2020. The first report on the source-to-sink characterization of microplastic pollution from a riverine environment in tropical India. Sci. Total Environ. 739, 140377.
- Baechler, B.R., Granek, E.F., Hunter, M.V., Conn, K.E., 2020. Microplastic concentrations in two Oregon bivalve species: spatial, temporal, and species variability. Limnol. Oceanogr. Lett. 5 (1), 54–65.
- Baldwin, A.K., Corsi, S.R., Mason, S.A., 2016. Plastic debris in 29 Great Lakes tributaries: relations to watershed attributes and hydrology. Environ. Sci. Technol. 50 (19), 10377–10385.
- Baldwin, A.K., Spanjer, A.R., Rosen, M.R., Thom, T., 2020. Microplastics in Lake Mead National Recreation Area, USA: occurrence and biological uptake. PLoS One 15 (5), e0228896 San Francisco.
- Ballent, A., Corcoran, P.L., Madden, O., Helm, P.A., Longstaffe, F.J., 2016. Sources and sinks of microplastics in Canadian Lake Ontario nearshore, tributary and beach sediments. Mar. Pollut. Bull. 110 (1), 383–395.
- Barrows, A.P.W., Christiansen, K.S., Bode, E.T., Hoellein, T.J., 2018. A watershed-scale, citizen science approach to quantifying microplastic concentration in a mixed land-use river. Water Res. 147, 382–392.
- Battulga, B., Kawahigashi, M., Oyuntsetseg, B., 2019. Distribution and composition of plastic debris along the river shore in the Selenga River basin in Mongolia. Environ. Sci. Pollut. Res. 26 (14), 14059–14072.
- Belen Alfonso, M., Scordo, F., Seitz, C., Mavo Manstretta, G.M., Carolina Ronda, A., Hugo Arias, A., Pablo Tomba, J., Ignacio Silva, L., Eduardo Perillo, G.M., Cintia Piccolo, M., 2020. First evidence of microplastics in nine lakes across Patagonia (South America). Sci. Total Environ. 733, 139385.
- Bertoldi, C., Lara, L.Z., Martins, F.C.G., Battisti, M.A., Hinrichs, R., Fernandes, A.N., 2021. First evidence of microplastic contamination in the freshwater of Lake Guaíba, Porto Alegre, Brazil. Sci. Total Environ. 759, 143503.
- Brander, S.M., Renick, V.C., Foley, M.M., Steele, C., Woo, M., Lusher, A., Carr, S., Helm, P., Box, C., Cherniak, S., Andrews, R.C., Rochman, C.M., 2020. Sampling and quality assurance and quality control: a guide for scientists investigating the occurrence of microplastics across matrices. Appl. Spectrosc. 74 (9), 1099–1125.
- Bujaczek, T., Kolter, S., Locky, D., Ross, M.S., 2021. Characterization of microplastics and anthropogenic fibers in surface waters of the North Saskatchewan River, Alberta, Canada. FACETS 6, 26–43.

- Bureau of Environmental Services, City of Portlandcollab, 2021. City of Portland HYDRA Rainfall Network. https://or.water.usgs.gov/non-usgs/bes/precip.html. (Accessed 15 August 2021) UNSP 125486.
- Campanale, C., Savino, I., Pojar, I., Massarelli, C., Uricchio, V.F., 2020a. A practical overview of methodologies for sampling and analysis of microplastics in riverine environments. Sustainability 12 (17), 6755.
- Campanale, C., Stock, F., Massarelli, C., Kochleus, C., Bagnuolo, G., Reifferscheid, G., Uricchio, V.F., 2020b. Microplastics and their possible sources: the example of ofanto river in Southeast Italy. Environ. Pollut. 258, 113284.
- Campbell, S.H., Williamson, P.R., Hall, B.D., 2017. Microplastics in the gastrointestinal tracts of fish and the water from an urban prairie creek ed. D. Schindler. FACETS 2 (1), 395–409
- Carpenter, E.J., Smith, K.L., 1972. Plastics on the Sargasso Sea surface. Science 175 (4027), 1240–1241.
- de Carvalho, A.R., Garcia, F., Riem-Galliano, L., Tudesque, L., Albignac, M., ter Halle, A., Cucherousset, J., 2021. Urbanization and hydrological conditions drive the spatial and temporal variability of microplastic pollution in the Garonne River. Sci. Total Environ. 769, 144479.
- Chang, H., Allen, D., Morse, J., Mainali, J., 2019. Sources of contaminated flood sediments in a rural-urban catchment: Johnson Creek, Oregon. J. Flood Risk Manag. 12 (4), e12496.
- Chen, H.J., Chang, H., 2014. Response of discharge, TSS, and E. coli to rainfall events in urban, suburban, and rural watersheds. Environ Sci Process Impacts 16 (10), 2313–2324.
- Chen, J., Chang, H., 2019. Dynamics of wet-season turbidity in relation to precipitation, discharge, and land cover in three urbanizing watersheds, Oregon. River Res. Appl. 35 (7), 892–904.
- Chen, H., Jia, Q., Zhao, X., Li, L., Nie, Y., Liu, H., Ye, J., 2020. The occurrence of microplastics in water bodies in urban agglomerations: impacts of drainage system overflow in wet weather, catchment land-uses, and environmental management practices. Water Res. 183, 116073.
- Cheung, P.K., Hung, P.L., Fok, L., 2019. River microplastic contamination and dynamics upon a rainfall event in Hong Kong, China. Environ. Process. 6 (1), 253–264.
- Constant, M., Ludwig, W., Kerherve, P., Sola, J., Charriere, B., Sanchez-Vidal, A., Canals, M., Heussner, S., 2020. Microplastic fluxes in a large and a small Mediterranean river catchments: the tet and the rhone, northwestern Mediterranean Sea. Sci. Total Environ. 716, 136984.
- Cowger, W., Steinmetz, Z., Gray, A., Munno, K., Lynch, J., Hapich, H., Primpke, S., De Frond, H., Rochman, C., Herodotou, O., 2021. Microplastic spectral classification needs an open source community: open specy to the rescue! Anal. Chem. 93 (21), 7543–7548.
- Di, M., Wang, J., 2018. Microplastics in surface waters and sediments of the three gorges reservoir, China. Sci. Total Environ. 616, 1620–1627.
- Dikareva, N., Simon, K.S., 2019. Microplastic pollution in streams spanning an urbanisation gradient. Environ. Pollut. 250, 292–299.
- Dris, R., Gasperi, J., Rocher, V., Tassin, B., 2018. Synthetic and non-synthetic anthropogenic fibers in a river under the impact of Paris megacity: sampling methodological aspects and flux estimations. Sci. Total Environ. 618, 157–164.
- Edo, C., González-Pleiter, M., Leganés, F., Fernández-Piñas, F., Rosal, R., 2020. Fate of microplastics in wastewater treatment plants and their environmental dispersion with effluent and sludge. Environ. Pollut. 259, 113837.
- Eo, S., Hong, S.H., Song, Y.K., Han, G.M., Shim, W.J., 2019. Spatiotemporal distribution and annual load of microplastics in the Nakdong River, South Korea. Water Res. 160, 228–237.
- Estahbanati, S., Fahrenfeld, N.L., 2016. Influence of wastewater treatment plant discharges on microplastic concentrations in surface water. Chemosphere 162, 277–284.
- ESRI, 2020. ArcGIS Desktop: Release 10.8.1. Environmental Systems Research Institute, Redlands, CA.
- Fan, Y., Zheng, K., Zhu, Z., Chen, G., Peng, X., 2019. Distribution, sedimentary record, and persistence of microplastics in the Pearl River catchment, China. Environ. Pollut. 251, 862–870.
- Fan, J., Zou, L., Zhao, G., 2021. Microplastic abundance, distribution, and composition in the surface water and sediments of the Yangtze River along Chongqing City, China. J. Soils Sediments 21 (4), 1840–1851.
- Feng, S., Lu, H., Tian, P., Xue, Y., Lu, J., Tang, M., Feng, W., 2020. Analysis of microplastics in a remote region of the tibetan plateau: implications for natural environmental response to human activities. Sci. Total Environ. 739, 140087.
- Granek, E.F., Brander, S.M., Holland, E.B., 2020. Microplastics in aquatic organisms: improving understanding and identifying research directions for the next decade. Limnol. Oceanogr. Lett. 5 (1), 1–4.
- Grbić, J., Helm, P., Athey, S., Rochman, C.M., 2020. Microplastics entering northwestern Lake Ontario are diverse and linked to urban sources. Water Res. 174, 115623.
- Guerranti, C., Cannas, S., Scopetani, C., Fastelli, P., Cincinelli, A., Renzi, M., 2017. Plastic litter in aquatic environments of Maremma Regional Park (Tyrrhenian Sea, Italy): contribution by the ombrone river and levels in marine sediments. Mar. Pollut. Bull. 117 (1), 366–370.
- Han, M., Niu, X., Tang, M., Zhang, B.-T., Wang, G., Yue, W., Kong, X., Zhu, J., 2020. Distribution of microplastics in surface water of the lower Yellow River near estuary. Sci. Total Environ. 707, 135601.
- Harris, L.S.T., Beur, L.La, Olsen, A.Y., Smith, A., Eggers, L., Pedersen, E., Brocklin, J.Van, Brander, S.M., Larson, S., 2022. Temporal variability of microparticles under the Seattle Aquarium, Washington State: documenting the global covid-19 pandemic. Environ. Toxicol. Chem. 41 (4), 917–930. https://doi.org/10.1002/etc.5190.
- He, B., Goonetilleke, A., Ayoko, G.A., Rintoul, L., 2020. Abundance, distribution patterns, and identification of microplastics in Brisbane River sediments, Australia. Sci. Total Environ. 700, 134467.
- Hitchcock, J.N., 2020. Storm events as key moments of microplastic contamination in aquatic ecosystems. Sci. Total Environ. 734, 139436.
- Hoellein, T.J., McCormick, A.R., Hittie, J., London, M.G., Scott, J.W., Kelly, J.J., 2017. Longitudinal patterns of microplastic concentration and bacterial assemblages in surface and benthic habitats of an urban river. Freshw. Sci. 36 (3), 491–507.

- Hu, D., Zhang, Y., Shen, M., 2020. Investigation on microplastic pollution of dongting Lake and its affiliated rivers. Mar. Pollut. Bull. 160, 111555.
- Huang, Y., Tian, M., Jin, F., Chen, M., Liu, Z., He, S., Li, F., Yang, L., Fang, C., Mu, J., 2020.
 Coupled effects of urbanization level and dam on microplastics in surface waters in a coastal watershed of Southeast China. Mar. Pollut. Bull. 154, 111089.
- Hurley, R., Woodward, J., Rothwell, J.J., 2018. Microplastic contamination of river beds significantly reduced by catchment-wide flooding. Nat. Geosci. 11 (4), 251–257.
- Jiang, C., Yin, L., Li, Z., Wen, X., Luo, X., Hu, S., Yang, H., Long, Y., Deng, B., Huang, L., Liu, Y., 2019. Microplastic pollution in the rivers of the Tibet plateau. Environ. Pollut. 249, 91–98.
- Kapp, K.J., Yeatman, E., 2018. Microplastic hotspots in the Snake and lower Columbia rivers: a journey from the greater yellowstone ecosystem to the Pacific Ocean. Environ. Pollut. 241, 1082–1090.
- Kataoka, T., Nihei, Y., Kudou, K., Hinata, H., 2019. Assessment of the sources and inflow processes of microplastics in the river environments of Japan. Environ. Pollut. 244, 958–965.
- Klasios, N., De Frond, H., Miller, E., Sedlak, M., 2021. Microplastics and other anthropogenic particles are prevalent in mussels from San Francisco Bay, and show no correlation with PAHs. Environ. Pollut. 271, 116260.
- Lahens, L., Strady, E., Kieu-Le, T.-C., Dris, R., Boukerma, K., Rinnert, E., Gasperi, J., Tassin, B., 2018. Macroplastic and microplastic contamination assessment of a tropical river (Saigon River, Vietnam) transversed by a developing megacity. Environ. Pollut. 236, 661–671.
- Leslie, H.A., Brandsma, S.H., van Velzen, M.J.M., Vethaak, A.D., 2017. Microplastics en route: field measurements in the dutch river delta and Amsterdam canals, wastewater treatment plants, North Sea sediments and biota. Environ. Int. 101, 133–142.
- Li, C., Busquets, R., Campos, L.C., 2020. Assessment of microplastics in freshwater systems: a review. Sci. Total Environ. 707, 135578.
- Ma, M., Liu, S., Su, M., Wang, C., Ying, Z., Huo, M., Lin, Y., Yang, W., 2021. Spatial distribution and potential sources of microplastics in the Songhua river flowing through urban centers in northeast China. Environ. Pollut. 118384.
- Mai, Y., Peng, S., Lai, Z., Wang, X., 2021. Measurement, quantification, and potential risk of microplastics in the mainstream of the Pearl River (Xijiang River) and its estuary, southern China. Environ. Sci. Pollut. Res. 28 (38), 53127–53140.
- Mainali, J., Chang, H., 2018. Landscape and anthropogenic factors affecting spatial patterns of water quality trends in a large river basin, South Korea. J. Hydrol. 564, 26–40.
- Mani, T., Hauk, A., Walter, U., Burkhardt-Holm, P., 2015. Microplastics profile along the Rhine River. Sci. Rep. 5 (1), 1–7.
- Mao, R., Hu, Y., Zhang, S., Wu, R., Guo, X., 2020. Microplastics in the surface water of wuliangsuhai Lake, northern China. Sci. Total Environ. 723, 137820.
- McCormick, A.R., Hoellein, T.J., London, M.G., Hittie, J., Scott, J.W., Kelly, J.J., 2016. Microplastic in surface waters of urban rivers: concentration, sources, and associated bacterial assemblages. Ecosphere 7 (11), e01556.
- Miller, R.Z., Watts, A.J.R., Winslow, B.O., Galloway, T.S., Barrows, A.P.W., 2017. Mountains to the sea: river study of plastic and non-plastic microfiber pollution in the Northeast USA. Mar. Pollut. Bull. 124 (1), 245–251.
- Mishell Donoso, J., Rios-Touma, B., 2020. Microplastics in tropical andean rivers: a perspective from a highly populated ecuadorian basin without wastewater treatment. Heliyon 6 (7), e04302.
- Mishra, Sujata, Swain, S., Sahoo, M., Mishra, Sunanda, Das, A.P., 2021. Geomicrobiol. J. https://doi.org/10.1080/01490451.2021.1983670.
- Multi-Resolution Land Characteristics Consortium, 2021. National Land Cover Dataset 2019 [11 August 2021].
- Natural Resources Conservation Service, 2021. United States Department of Agriculture Web Soil Survey [8 November 2021].
- Ogle, D.H., Doll, J.C., Wheeler, P., Dinno, A., 2021. FSA: Fisheries Stock Analysis. R package version 0.9.1. https://github.com/droglenc/FSA.
- Park, T.-J., Lee, S.-H., Lee, M.-S., Lee, J.-K., Park, J.-H., Zoh, K.-D., 2020. Distributions of microplastics in surface water, fish, and sediment in the vicinity of a sewage treatment plant. Water 12 (12), 3333.
- Parker, B.W., Beckingham, B.A., Ingram, B.C., Ballenger, J.C., Weinstein, J.E., Sancho, G., 2020. Microplastic and tire wear particle occurrence in fishes from an urban estuary: Influence of feeding characteristics on exposure risk. Mar. Pollut. Bull. 160, 111539.
- Peller, J.R., Eberhardt, L., Clark, R., Nelson, C., Kostelnik, E., Iceman, C., 2019. Tracking the distribution of microfiber pollution in a southern Lake Michigan watershed through the analysis of water, sediment and air. Environ Sci Process Impacts 21 (9), 1549–1559.
- Pratt, B., Chang, H., 2012. Effects of land cover, topography, and built structure on seasonal water quality at multiple spatial scales. J. Hazard. Mater. 209–210, 48–58.
- Primpke, S., Christiansen, S.H., Cowger, W., De Frond, H., Deshpande, A., Fischer, M., Holland, E.B., Meyns, M., O'Donnell, B.A., Ossmann, B.E., Pittroff, M., Sarau, G., Scholz-Böttcher, B.M., Wiggin, K.J., 2020. Critical assessment of analytical methods for the harmonized and cost-efficient analysis of microplastics. Appl. Spectrosc. 74 (9), 1012–1047
- Qin, Y., Wang, Z., Li, W., Chang, X., Yang, J., Yang, F., 2020. Microplastics in the sediment of Lake Ulansuhai of Yellow River Basin, China. Water Environ. Res. 92 (6), 829–839.
- R Core Team, 2021. R: A language and environment for statistical computing. R Foundation for Statistical Computing, Vienna, Austria. https://www.R-project.org/.
- Sang, W., Chen, Z., Mei, L., Hao, S., Zhan, C., bin Zhang, W., Li, M., Liu, J., 2021. The abundance and characteristics of microplastics in rainwater pipelines in Wuhan, China. Sci. Total Environ. 755, 142606.
- Sarkar, Deepayan, 2008. Lattice: Multivariate Data Visualization With R. Springer, New York 978-0-387-75968-5.
- Sarkar, D.J., Das Sarkar, S., Das, B.K., Manna, R.K., Behera, B.K., Samanta, S., 2019. Spatial distribution of meso and microplastics in the sediments of river ganga at eastern India. Sci. Total Environ. 694, 133712.
- Schmidt, L.K., Bochow, M., Imhof, H.K., Oswald, S.E., 2018. Multi-temporal surveys for microplastic particles enabled by a novel and fast application of SWIR imaging spectroscopy – study of an urban watercourse traversing the city of Berlin, Germany. Environ. Pollut. 239, 579–589.

- Shruti, V.C., Jonathan, M.P., Rodriguez-Espinosa, P.F., Rodríguez-González, F., 2019. Microplastics in freshwater sediments of Atoyac River basin, Puebla City, Mexico. Sci. Total Environ. 654, 154–163.
- Stanton, T., Johnson, M., Nathanail, P., MacNaughtan, W., Gomes, R.L., 2020. Freshwater microplastic concentrations vary through both space and time. Environ. Pollut. 263, 114481.
- Strady, E., Kieu-Le, T.-C., Gasperi, J., Tassin, B., 2020. Temporal dynamic of anthropogenic fibers in a tropical river-estuarine system. Environ. Pollut. 259, 113897.
- Talbot, R., Chang, H., 2022. Microplastics in freshwater: a global review of factors affecting spatial and temporal variations. Environ. Pollut. 292, 118393.
- Tian, Z., Zhao, H., Peter, K.T., Gonzalez, M., Wetzel, J., Wu, C., Hu, X., Prat, J., Mudrock, E., Hettinger, R., Cortina, A.E., Biswas, R.G., Kock, F.V.C., Soong, R., Jenne, A., Du, B., Hou, F., He, H., Lundeen, R., Gilbreath, A., Sutton, R., Scholz, N.L., Davis, J.W., Dodd, M.C., Simpson, A., McIntyre, J.K., Kolodziej, E.P., 2021. A ubiquitous tire rubber-derived chemical induces acute mortality in coho salmon. Science 371 (6525), 185–189.
- Tibbetts, J., Krause, S., Lynch, I., Smith, G.H.S., 2018. Abundance, distribution, and drivers of microplastic contamination in Urban River environments. Water 10 (11), 1597.
- Townsend, K.R., Lu, H.-C., Sharley, D.J., Pettigrove, V., 2019. Associations between microplastic pollution and land use in urban wetland sediments. Environ. Sci. Pollut. Res. 26 (22), 22551–22561.
- USGS Water Data for the Nation, 2021. National Water Information System (NWIS).
- Valine, A.E., Peterson, A.E., Horn, D.A., Scully-Engelmeyer, K.M., Granek, E.F., 2020. Microplastic prevalence in 4 Oregon Rivers along a rural to urban gradient applying a cost-effective validation technique. Environ. Toxicol. Chem. 39 (8), 1590–1598.
- Vu, Vincent Q., 2011. ggbiplot: A ggplot2 based biplot. R package version 0.55. http://github.com/vqv/ggbiplot.
- Wang, G., Lu, J., Tong, Y., Liu, Z., Zhou, H., Xiayihazi, N., 2020. Occurrence and pollution characteristics of microplastics in surface water of the Manas River Basin, China. Sci. Total Environ. 710, 136099.
- Wang, G., Lu, J., Li, W., Ning, J., Zhou, L., Tong, Y., Liu, Z., Zhou, H., Xiayihazi, N., 2021. Seasonal variation and risk assessment of microplastics in surface water of the Manas River Basin, China. Ecotoxicol. Environ. Saf. 208, 111477.
- Watkins, L., Sullivan, P.J., Walter, M.T., 2019. A case study investigating temporal factors that influence microplastic concentration in streams under different treatment regimes. Environ. Sci. Pollut. Res. 26 (21), 21797–21807.

- Wei, T., Simko, V., 2021. R package 'corrplot': Visualization of a Correlation Matrix (Version 0.90). Available from https://github.com/taiyun/corrplot.
- Werbowski, L.M., Gilbreath, A.N., Munno, K., Zhu, X., Grbic, J., Wu, T., Sutton, R., Sedlak, M.D., Deshpande, A.D., Rochman, C.M., 2021. Urban stormwater runoff: a major pathway for anthropogenic particles, black rubbery fragments, and other types of microplastics to urban receiving waters. ACS ES&T Water 1 (6), 1420–1428.
- Wickham, H., 2011. The Split-apply-combine strategy for data analysis. J. Stat. Softw. 40 (1), 1–29. http://www.istatsoft.org/v40/i01/.
- Wik, A., Dave, G., 2009. Occurrence and effects of tire wear particles in the environment a critical review and an initial risk assessment. Environ. Pollut. 157, 1–11.
- Wong, G., Löwemark, L., 2020. Microplastic pollution of the Tamsui River and its tributaries in northern Taiwan: spatial heterogeneity and correlation with precipitation. Environ. Pollut. 260, 113935.
- Wu, P., Tang, Y., Dang, M., Wang, S., Jin, H., Liu, Y., Jing, H., Zheng, C., Yi, S., Cai, Z., 2020. Spatial-temporal distribution of microplastics in surface water and sediments of Maozhou River within Guangdong-Hong Kong-Macao Greater Bay Area. Sci. Total Environ. 717, 135187.
- Xia, W., Rao, Q., Deng, X., Chen, J., Xie, P., 2020. Rainfall is a significant environmental factor of microplastic pollution in inland waters. Sci. Total Environ. 732, 139065.
- Xiong, X., Wu, C., Elser, J.J., Mei, Z., Hao, Y., 2019. Occurrence and fate of microplastic debris in middle and lower reaches of the Yangtze River – from inland to the sea. Sci. Total Environ. 659, 66–73.
- Yin, L., Wen, X., Du, C., Jiang, J., Wu, L., Zhang, Y., Hu, Z., Hu, S., Feng, Z., Zhou, Z., Long, Y., Gu, Q., 2020. Comparison of the abundance of microplastics between rural and urban areas: a case study from East Dongting Lake. Chemosphere 244 UNSP 125486.
- Yonkos, L.T., Friedel, E.A., Perez-Reyes, A.C., Ghosal, S., Arthur, C.D., 2014. Microplastics in four estuarine rivers in the Chesapeake Bay, U.S.A. Environ. Sci. Technol. 48 (24), 14195–14202.
- Zhao, S., Wang, T., Zhu, L., Xu, P., Wang, X., Gao, L., Li, D., 2019. Analysis of suspended microplastics in the changjiang estuary: implications for riverine plastic load to the ocean. Water Res. 161, 560–569.
- Zhou, G., Wang, Q., Zhang, J., Li, Q., Wang, Y., Wang, M., Huang, X., 2020. Distribution and characteristics of microplastics in urban waters of seven cities in the Tuojiang River basin, China. Environ. Res. 189. 109893.